Available online at www.sciencedirect.com
SCIENCE DIRECT®
Journal of Magnetism and Magnetic Materials 290–291 (2005) 1304–1308
Journal of magnetism and magnetic materials
www.elsevier.com/locate/jmmm

# Formulas for computing the magnetic flux density of fine magnetic pole pitch fabricated on printed circuit board

Kuo-Chi Chiu[a,b,*], Der-Ray Huang[b], Han-Ping D. Shieh[a]

[a]Department of Photonics & Institute of Electro-Optical Engineering, Chiao Tung University, Hsinchu 300, Taiwan
[b]Industrial Technology Research Institute (ITRI), Building 78, J011, 195, Section 4, Chung Hsing Road, Chutung, Hsinchu 310, Taiwan

Available online 15 December 2004

## Abstract

A special wire circuit with an appropriate layout was designed and formed on printed circuit board (PCB). After a current flowed through the wire circuit, the magnetic field was induced according to Ampere's law and a fine magnetic pole pitch of less than 1 mm was fabricated. Three-dimensional formulas are presented for computing the magnetic flux density of fine magnetic pole pitch fabricated on PCB. These formulas are expressed in terms of finite sums of elementary functions and enable rapid parametric studies of the magnetic flux density distribution relative to wire width, wire thickness, dimension of magnetic pole pitch, etc. They are easily programmed and have been successfully verified by experimental measurements.


*PACS:* 41.20.Gz; 85.70.Ay

*Keywords:* Printed circuit board (PCB); Pole pitch; Magnetization; Magnetic encoder

## 1. Introduction

Magnetic encoder is widely used in detecting the rotation speed, position and angle in many precise control systems. It consists of a magnetic reading device and a multi-pole magnetic component with fine magnetic pole pitch. The resolution can be improved effectively by narrowing the magnetic pole pitch. Using the traditional methods, the magnetic pole pitch of less than 1 mm was very difficult to be achieved and a costly complicated magnetization system was required [1,2]. Fine magnetic pole pitches of less than 1 mm can be easily fabricated by using PCB technology and it has been investigated possessing of a periodic structure as shown in Fig. 1.

In this paper, three-dimensional analytical expressions are derived for computing the magnetic flux density of fine magnetic pole pitch fabricated on PCB. The analysis is based on the assumption of a current with a uniform density flowing through the wire circuit. The formulas are given in terms of elementary functions and are readily programmed. They are suitable for parametric design and optimization.

## 2. Theory

Several techniques can be used for computing the magnetic flux density of fine magnetic pole pitch fabricated on PCB due to the current induced. Here is

*Corresponding author. Tel.: +886 3 5913530; fax: +886 3 5832805.
*E-mail address:* kuochi@itri.org.tw (K.-C. Chiu).

0304-8853/$ - see front matter 
doi:10.1016/j.jmmm.2004.11.424

to model the wire circuit as distributions of uniform current density and then compute the magnetic flux density. According to Biot–Savart law [3], a finite length $L$ and straight wire carrying a steady current $I$ as shown in Fig. 2a, the magnetic flux density at a point $P$ with a distance $r$ is given by

$$\vec{B} = \frac{\mu_0 I}{4\pi r}\left(\frac{a}{\sqrt{a^2+r^2}} + \frac{b}{\sqrt{b^2+r^2}}\right)\hat{\phi}, \quad (1)$$

where $\mu_0$ is the permeability of free space.

Actually, the cross-section of circuit wire on PCB is not circular but rectangular which can be discretized into a mesh of indexed elements as shown in Fig. 2b. These elements are equal in area containing the same amount of current density. Both wire width $T1$ and wire thickness $T2$ should be considered when $T1 \approx r$ and $T2 \approx r$. Each small element is a finite length and straight wire and therefore the magnetic flux density can be calculated by Eq. (1). After summing the contribution of each element, the total magnetic flux density $\vec{B}$ in $z$ component is given by

$$Bz = \sum_{n1=1}^{m1}\sum_{n2=1}^{m2} \frac{\mu_0 i}{4\pi R_{n1,n2}} \times \left(\frac{a}{\sqrt{a^2+R_{n1,n2}^2}} + \frac{b}{\sqrt{b^2+R_{n1,n2}^2}}\right)\sin\theta, \quad (2)$$

where $n1$ and $n2$ are intergers, $m1$ and $m2$ are "mesh" parameters that characterize the discretization of the cross-section of wire and $\theta$ is the angular offset of $x$-axis. The paramters of $i$, $R_{n1,n2}$ and $\sin\theta$ are given by

$$i = \frac{I}{m1m2}, \quad R_{n1,n2} = \sqrt{r_{n1}^2 + z_{n2}^2}, \quad \sin\theta = r_{n1}/R_{n1,n2}, \quad (3)$$

$$r_{n1} = \left(r - \frac{n1}{m1}T1\right), \quad z_{n2} = \left(z - \frac{n2}{m2}T2\right) \quad (n1 \sim m1, n2 \sim m2). \quad (4)$$

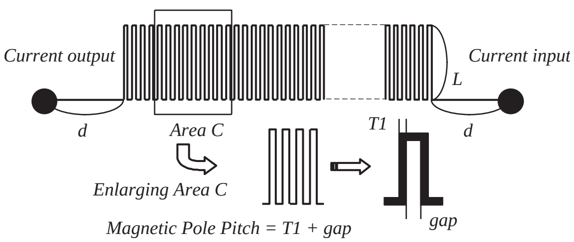

Fig. 1. Special wire circuit with a periodic structure on PCB.

The wire circuit fabricated on PCB in Fig. 1 can be redrawn as shown in Fig. 3. Each part can be treated as a finite length and straight wire carring a steady current and therefore the magnetic flux density can be calculated by Eq. (2). Consequently, the total magnetic flux density at any position on PCB can be acquired after accumulating all contributions of each part. As a result, the magnetic flux density in $z$ component on the central

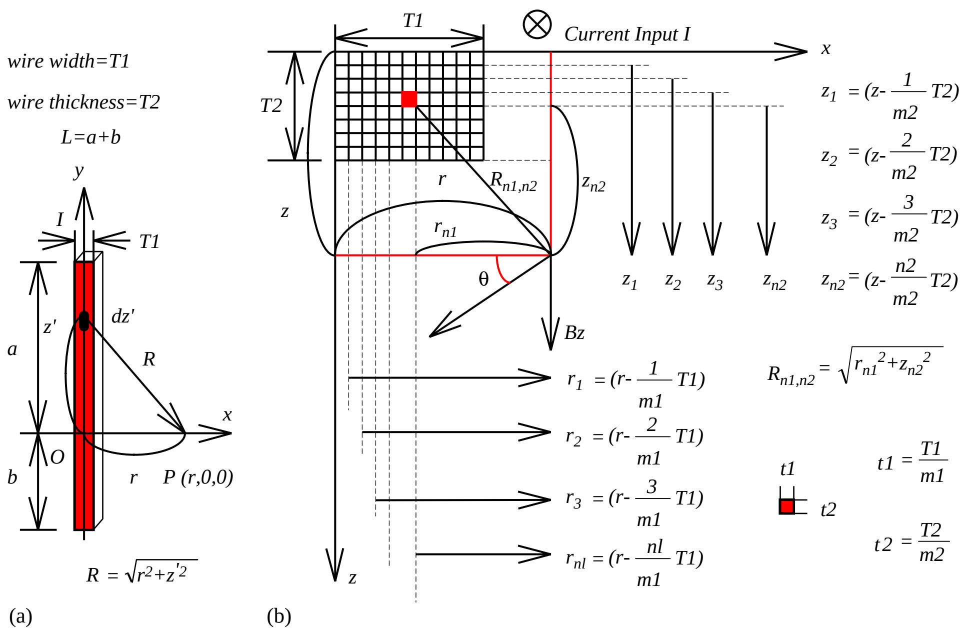

Fig. 2. Mesh of cross-section at a circuit wire on PCB.

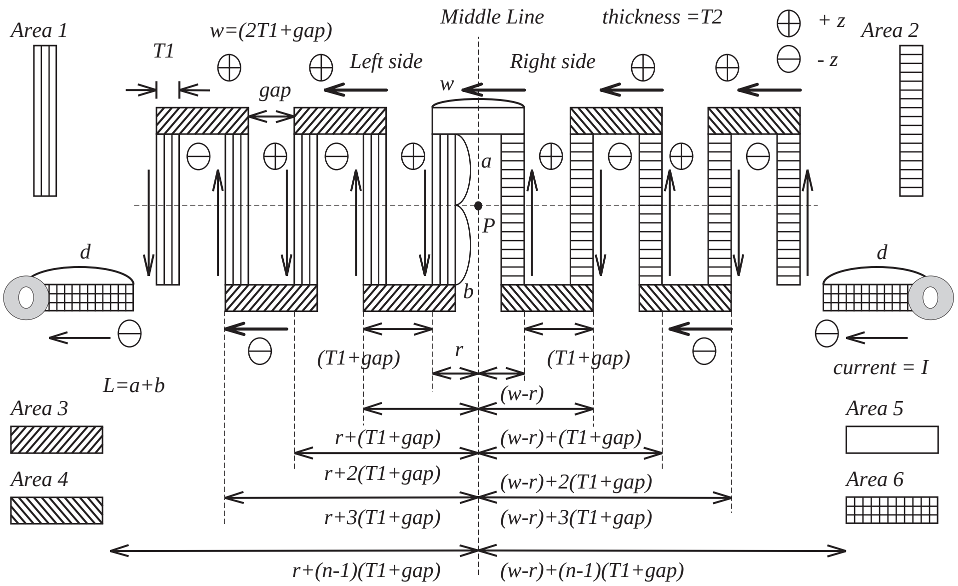


Fig. 3. Geometrical structure and dimension of wire circuit.

pole from all areas in Fig. 3 can be obtained after superposition.

At Area 1, the contribution of $Bz\_A1$ is given by

$$Bz\_A1 = \sum_{n=1}^{m}\sum_{n2=1}^{m2}\sum_{n1=1}^{m1} \frac{\mu_0 i}{4\pi R\_A1} \times \left( \frac{a}{\sqrt{a^2 + R\_A1^2}} + \frac{b}{\sqrt{b^2 + R\_A1^2}} \right) \times \sin\theta\_A1 \times (-1)^{n-1} \quad (n = 1 \sim m), \tag{5}$$

$$R\_A1 = \sqrt{r\_A1^2 + z\_A1^2}, \quad \sin\theta\_A1 = r\_A1/R\_A1, \tag{6}$$

$$r\_A1 = \left(r - \frac{n1}{m1}\,T1\right) + (n-1)(T1 + \mathrm{gap}), \quad z\_A1 = z - \frac{n2}{m2}\,T2, \tag{7}$$

where $n$ is an integer and $m$ is the number of wire.

At Area 2, the contribution of $Bz\_A2$ is given by

$$Bz\_A2 = \sum_{n=1}^{m}\sum_{n2=1}^{m2}\sum_{n1=1}^{m1} \frac{\mu_0 i}{4\pi R\_A2} \times \left( \frac{a}{\sqrt{a^2 + R\_A2^2}} + \frac{b}{\sqrt{b^2 + R\_A2^2}} \right) \times \sin\theta\_A2 \times (-1)^{n-1} \quad (n = 1 \sim m), \tag{8}$$

$$R\_A2 = \sqrt{r\_A2^2 + z\_A2^2}, \quad \sin\theta\_A2 = r\_A2/R\_A2, \tag{9}$$

$$r\_A2 = \left[(w-r) - \frac{n1}{m1}\,T1\right] + (n-1)(T1 + \mathrm{gap}), \tag{10}$$

$$z\_A2 = z - \frac{n2}{m2}\,T2, \quad w = (2T1 + \mathrm{gap}). \tag{11}$$

At Area 3 (on the top side), $Bz\_A3t$ is given by

$$Bz\_A3t = \sum_{n=3}^{m}\sum_{n2=1}^{m2}\sum_{n1=1}^{m1} \frac{\mu_0 i}{4\pi R\_A3t} \times \left( \frac{h\_A3t}{\sqrt{h\_A3t^2 + R\_A3t^2}} - \frac{h\_A3t - w}{\sqrt{(h\_A3t - w)^2 + R\_A3t^2}} \right) \times \sin\theta\_A3t \times (+1), \tag{12}$$

$$R\_A3t = \sqrt{r\_A3t^2 + z\_A3t^2}, \quad \sin\theta\_A3t = r\_A3t/R\_A3t, \tag{13}$$

$$r\_A3t = (T1 + a) - \frac{n1}{m1}\,T1, \quad z\_A3t = z - \frac{n2}{m2}\,T2, \tag{14}$$

$$h\_A3t = r + (n-1)(T1 + \mathrm{gap}) \quad (n = 3, 5, 7, \ldots, m). \tag{15}$$

At Area 3 (on the bottom side), $Bz\_A3b$ is given by

$$Bz\_A3b = \sum_{n=2}^{m}\sum_{n2=1}^{m2}\sum_{n1=1}^{m1}\frac{\mu_0 i}{4\pi R\_A3b}\eta \times\left(\frac{h\_A3b}{\sqrt{h\_A3b^2+R\_A3b^2}} - \frac{h\_A3b-w}{\sqrt{(h\_A3b-w)^2+R\_A3b^2}}\right) \times \sin\theta\_A3b\times(-1), \quad (16)$$

$$R\_A3b=\sqrt{r\_A3b^2+z\_A3b^2}, \quad \sin\theta\_A3b = r\_A3b/R\_A3b, \quad (17)$$

$$r\_A3b=(T1+b)-\frac{n1}{m1}T1, \quad z\_A3b = z-\frac{n2}{m2}T2, \quad (18)$$

$$h\_A3b = r+(n-1)(T1+\text{gap}) \quad (n=2,4,6,\dots,m). \quad (19)$$

At Area 4 (on the top side), $Bz\_A4t$ is given by

$$Bz\_A4t = \sum_{n=3}^{m}\sum_{n2=1}^{m2}\sum_{n1=1}^{m1}\frac{\mu_0 i}{4\pi R\_A4t} \times\left(\frac{h\_A4t}{\sqrt{h\_A4t^2+R\_A4t^2}} - \frac{h\_A4t-w}{\sqrt{(h\_A4t-w)^2+R\_A4t^2}}\right) \times \sin\theta\_A4t\times(+1), \quad (20)$$

$$R\_A4t=\sqrt{r\_A4t^2+z\_A4t^2}, \quad \sin\theta\_A4t = r\_A4t/R\_A4t, \quad (21)$$

$$r\_A4t=(T1+a)-\frac{n1}{m1}T1, \quad z\_A4t = z-\frac{n2}{m2}T2, \quad (22)$$

$$h\_A4t = (w-r)+(n-1)(T1+\text{gap}) \quad (n=3,5,7,\dots,m). \quad (23)$$

At Area 4 (on the bottom side), $Bz\_A4b$ is given by

$$Bz\_A4b = \sum_{n=2}^{m}\sum_{n2=1}^{m2}\sum_{n1=1}^{m1}\frac{\mu_0 i}{4\pi R\_A4b} \times\left(\frac{h\_A4b}{\sqrt{h\_A4b^2+R\_A4b^2}} - \frac{h\_A4b-w}{\sqrt{(h\_A4b-w)^2+R\_A4b^2}}\right) \times \sin\theta\_A4b\times(-1), \quad (24)$$

$$R\_A4b=\sqrt{r\_A4b^2+z\_A4b^2}, \quad \sin\theta\_A4b = r\_A4b/R\_A4b, \quad (25)$$

$$r\_A4b=(T1+b)-\frac{n1}{m1}T1, \quad z\_A4b = z-\frac{n2}{m2}T2, \quad (26)$$

$$h\_A4b = (w-r)+(n-1)(T1+\text{gap}) \quad (n=2,4,6,\dots,m). \quad (27)$$

At Area 5, the contribution of $Bz\_A5$ is given by

$$Bz\_A5 = \sum_{n2=1}^{m2}\sum_{n1=1}^{m1}\frac{\mu_0 i}{4\pi R\_A5}\left(\frac{w-r}{\sqrt{(w-r)^2+R\_A5^2}} + \frac{r}{\sqrt{r^2+R\_A5^2}}\right)\sin\theta\_A5, \quad (28)$$

$$R\_A5=\sqrt{r\_A5^2+z\_A5^2}, \quad \sin\theta\_A5 = r\_A5/R\_A5, \quad (29)$$

$$r\_A5=(T1+a)-\frac{n1}{m1}T1, \quad z\_A5 = z-\frac{n2}{m2}T2. \quad (30)$$

At Area 6 (on the left side), $Bz\_A6l$ is given by

$$Bz\_A6l = \sum_{n2=1}^{m2}\sum_{n1=1}^{m1}\frac{\mu_0 i}{4\pi R\_A6l} \times\left(\frac{h\_A6l}{\sqrt{h\_A6l^2+R\_A6l^2}} - \frac{h\_A6l-d}{\sqrt{(h\_A6l-d)^2+R\_A6l^2}}\right) \times \sin\theta\_A6l\times(-1), \quad (31)$$

$$R\_A6l = \sqrt{r\_A6l^2 + z\_A6l^2},$$
$$\sin\theta\_A6l = r\_A6l/R\_A6l, \tag{32}$$

$$r\_A6l = (T1 + b) - \frac{n1}{m1}T1,$$
$$z\_A6l = z - \frac{n2}{m2}T2, \tag{33}$$

$$h\_A6l = r + (m-1)(T1 + \text{gap}) + d. \tag{34}$$

At Area 6 (on the right side), $Bz\_A6r$ is given by

$$Bz\_A6r = \sum_{n2=1}^{m2}\sum_{n1=1}^{m1}\frac{\mu_0 i}{4\pi R\_A6r} \times \left(\frac{h\_A6r}{\sqrt{h\_A6r^2 + R\_A6r^2}} - \frac{h\_A6r - d}{\sqrt{(h\_A6r - d)^2 + R\_A6r^2}}\right) \times \sin\theta\_A6r \times (-1), \tag{35}$$

$$R\_A6r = \sqrt{r\_A6r^2 + z\_A6r^2},$$
$$\sin\theta\_A6r = r\_A6r/R\_A6r, \tag{36}$$

$$r\_A6r = (T1 + b) - \frac{n1}{m1}T1,$$
$$z\_A6r = z - \frac{n2}{m2}T2, \tag{37}$$

$$h\_A6r = (w - r) + (m-1)(T1 + \text{gap}) + d. \tag{38}$$

## 3. Experiments and results

Nine-pole magnetic components were fabricated on PCB with different wire width $T1$ and gap for making different magnetic pole pitches. The total magnetic flux density distributions in $z$ component on the central pole were measured as shown in Figs. 4 and 5. The circle and square marks denote for the distributions at the detection spacing of 200 and 300 μm above the surface, respectively. The measured values of magnetic flux density are in agreement with the calculated values.

## 4. Conclusions

Three-dimensional field formulas have been derived for computing the magnetic flux density of fine magnetic pole pitch fabricated on PCB. These field solutions are in terms of finite sums of elementary functions and enable rapid parametric studies of the magnetic flux density distribution relative to wire width, wire thickness, dimension of magnetic pole pitch, etc. They are easily programmed and have been verified by experimental measurements.

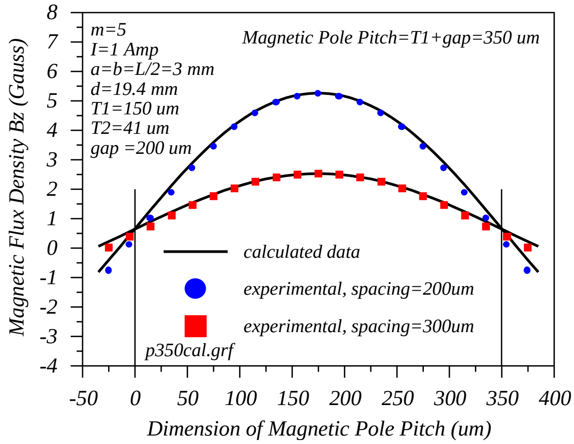


Fig. 4. Magnetic flux density distributions on the central pole at a fine magnetic pole pitch of 350 μm.

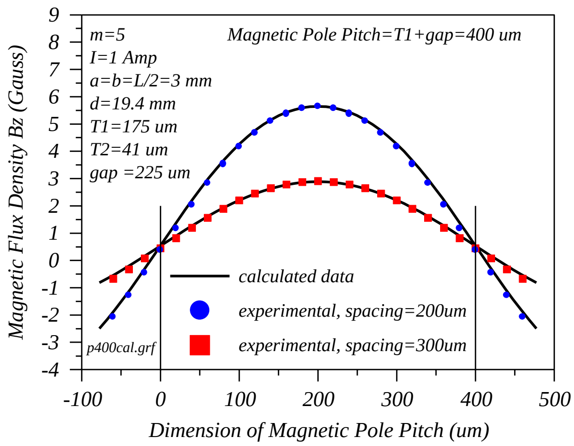


Fig. 5. Magnetic flux density distributions on the central pole at a fine magnetic pole pitch of 400 μm.

## References

[1] K. Miyashita, T. Takahashi, M. Yamanaka, IEEE Trans. Magn. 23 (1987) 2182.
[2] Y.J. Luo, E.T. Hwang, S.M. Huang, Proceedings of the EEIC/ICWA Exposition, USA, October 4–7, 1993, pp. 237–242.
[3] P. Lorran, et al., Electromagnetic Fields And Waves, third ed., Freeman Company, New York, 1988, pp. 327–337.